

# Near-wake of a perturbed, horizontal cylinder at a free-surface

J.-C. Lin, J. Sheridan,<sup>a)</sup> and D. Rockwell<sup>b)</sup>

*Department of Mechanical Engineering and Mechanics, 354 Packard Laboratory, 19 Memorial Drive West, Lehigh University, Bethlehem, Pennsylvania 18015*

(Received 17 October 1995; accepted 22 April 1996)

A horizontal cylinder intersecting a free surface is subjected to controlled vertical perturbations, and the consequent vortex formation is characterized by high-image-density particle image velocimetry, which leads to instantaneous patterns of velocity, vorticity, and streamlines. For the limiting case of the stationary cylinder, the near wake does not exhibit rapid formation of organized vortical structures in a manner similar to Kármán vortices. Application of perturbations, however, generates phase-locked vortex formation over a wide range of excitation frequencies, even at relatively low amplitudes, indicating that the near wake in presence of a free surface is convectively, rather than absolutely, unstable. At a sufficiently high value of excitation frequency, the formation of the initial vortex undergoes an abrupt change in timing, which is analogous to that occurring for Kármán vortex formation from a completely submerged cylinder. All of these features of the near wake are interpreted in terms of foci, saddle points, and reattachment points of the streamwise topology.  
© 1996 American Institute of Physics. [S1070-6631(96)02408-7]

## I. INTRODUCTION

Flow past a completely submerged cylinder has been a topic of intense interest in recent decades. An effective means of characterizing the near-wake structure is to subject the cylinder to controlled oscillations and observe the process of vortex formation using qualitative flow visualization. Koopman,<sup>1,2</sup> Griffin,<sup>3,4</sup> Griffin and Vortaw,<sup>5</sup> Ongoren and Rockwell,<sup>6</sup> and Cheng and Moretti<sup>7</sup> describe various aspects of the near wake. In all of these studies, the emphasis was on excitation frequencies near or at the inherent vortex formation frequency, and the concept of “lock-on” of the vortex formation relative to the cylinder motion was a central feature. Williamson and Roshko<sup>8</sup> consider a relatively wide range of excitation frequency and describe a diversity of locked-on vortex patterns in the near wake, in addition to classical lock-on. Griffin and Hall,<sup>9,10</sup> taking an overview of the lock-on process in their and previous studies, provide an insightful assessment of our current understanding.

When the cylinder is excited at a frequency close to that of the inherent Kármán vortex formation, large changes in the amplitude of the fluctuating lift coefficient  $\bar{C}_L$  and the phase  $\phi_L$  of this lift relative to the cylinder displacement can occur, as evident in the measurements of Bishop and Hassan,<sup>11</sup> Staubli,<sup>12</sup> and Sarpkaya.<sup>13</sup> Equivalently, similar trends are evident for measurements of fluctuating pressure on the surface of the cylinder, as in the investigations of Bearman and Currie,<sup>14</sup> Ferguson and Parkinson,<sup>15</sup> and Feng.<sup>16</sup> Even cylinders having a rectangular cross section, investigated by Bearman and Obasaju<sup>17</sup> and blunt trailing edges, addressed by Staubli and Rockwell<sup>18</sup> and Lotfy and Rockwell,<sup>19</sup> can exhibit large changes in magnitude and phase of the surface loading.

Central to understanding these changes in the loading is insight into the corresponding variations of the vortex forma-

tion process. Zdravkovich<sup>20</sup> first suggested that the change in phase of the cylinder loading was due to a change in timing of the initially formed vortex. Ongoren and Rockwell<sup>6</sup> further investigated this concept for cylinders of various cross-sectional geometries and quantitatively related changes in timing of the vortex formation to variations in phase of the velocity fluctuations. Williamson and Roshko<sup>8</sup> observed, for sufficiently large amplitude, not simply the Kármán vortices, but additional vortices having a sense opposite to the respective Kármán vortex. Gu, Chyu, and Rockwell<sup>21</sup> provide instantaneous, quantitative representations of the near-wake structure for small amplitude, on the basis of streamlines and vorticity distributions, show the mechanisms of the near wake leading to the switching in timing of the initially formed vortex.

In contrast to these extensive studies of the wake of a completely submerged cylinder, little is known of the near-wake structure from a partially submerged cylinder subjected to controlled oscillations. An important consequence of the free surface is, as indicated by the linear stability analysis of Triantafyllou and Dimas,<sup>22,23</sup> to preclude the onset of an absolute (global) instability. The near wake of a half-submerged cylinder is therefore not expected to exhibit organized vortex formation close to the base of the cylinder in the manner of classical Kármán shedding.

If the near wake is indeed convectively unstable, as shown in the analysis of Triantafyllou and Dimas,<sup>22,23</sup> then it should be highly sensitive to perturbations of the cylinder. The consequence of such perturbations has not been explored. Even small-amplitude perturbations may give rise to phase-locked vortex formation. A further question is whether, at a critical value of excitation frequency, there occurs an abrupt change in timing of the initially shed vortex. If so, it is desirable to establish the extent to which it is analogous to that of Kármán vortex formation from a completely submerged cylinder, as characterized by the vorticity patterns of Gu, Chyu, and Rockwell.<sup>21</sup> These aspects will be addressed using instantaneous distributions of velocity and

<sup>a)</sup>On leave from Monash University, Melbourne, Australia.

<sup>b)</sup>Corresponding author. Telephone: 610-758-4107; telefax: 610-758-4041; electronic mail: dor0@lehigh.edu

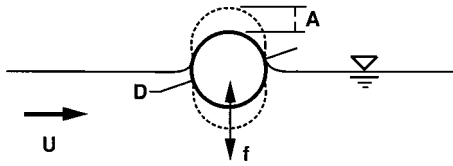


FIG. 1. Overview of experimental system and definition of flow and geometric parameters.

vorticity, as well as topological features of the instantaneous streamline patterns.

## II. EXPERIMENTAL SYSTEM AND TECHNIQUES

Experiments were performed in a water channel having a test section width of 210 mm and a depth of 527 mm. As shown in the schematic of Fig. 1, a cylinder of 25.4 mm diam was mounted horizontally. In its stationary, nominal position, the cylinder was half-submerged. A free-stream velocity of 112 mm/s provided a Reynolds number based on cylinder diameter  $D$  of 2855.

The cylinder was held in position by a vertical arm, which was isolated from the free stream by a false wall arrangement. A specially designed endplate ensured no leakage between the junction of the oscillating cylinder and the stationary, vertical wall. A high-resolution, computer-controlled motor generated the desired frequencies and amplitudes of the vertical perturbation of the cylinder. Frequencies  $f$  over the range  $0.5 \leq f \leq 2.0$  Hz were considered. The corresponding frequency  $f_0$  of Kármán vortex formation from the completely submerged cylinder at the same value of free-stream velocity is  $f_0 = 0.93$  Hz. The normalized excitation frequency  $f/f_0$  therefore extends over the range  $0.54 \leq f/f_0 \leq 2.15$ . Amplitudes  $A$  of the perturbation were  $1 \text{ mm} \leq A \leq 5 \text{ mm}$ , or, normalized with the cylinder diameter  $D$ ,  $0.04 \leq A/D \leq 0.20$ .

The instantaneous structure of the near wake of the cylinder was determined using a scanning laser version of high-image-density particle image velocimetry, described by Rockwell *et al.*<sup>24</sup> The beam from a 20 W continuous wave Argon-ion laser was directed at a rotating, polygonal mirror having 72 facets. This concept yielded a scanning frequency of 1252 Hz which, in essence, provided illumination equivalent to a pulsed laser sheet. The flow was seeded with metallic-coated, hollow glass particles having a diameter of 12  $\mu\text{m}$ . Images of the multiply exposed particles were recorded on high resolution 35 mm film. Subsequently, the negatives were digitized at a resolution of 125 pixels/mm. For interrogation windows having a size of 0.72 mm  $\times$  0.72 mm, the velocity vector was calculated using a single-frame, cross-correlation technique. The effective grid size in the physical plane of the laser sheet of 1.16 mm, based on the magnification of the camera lens, was 1:3.2.

Acquisition of instantaneous images was triggered with respect to the motion of the cylinder. In essence, two instants, one during the upstroke motion of the cylinder and the other during the downstroke motion, were of interest. The

criterion for the upstroke trigger was the cylinder position  $45^\circ$  after attainment of bottom dead center, and for the downstroke,  $45^\circ$  after top dead center.

## III. EFFECT OF CYLINDER PERTURBATIONS: PHASE-LOCKED STATES

Figure 2(a) shows the wake structure from the stationary cylinder, represented by an ensemble average of six images. The vorticity layer from the cylinder eventually “reattaches” to the free surface, as suggested by both the contours of constant vorticity and the velocity distributions. The general form of this so-called wake region of the cylinder is therefore in accord with that formulated by Triantafyllou and Dimas.<sup>22,23</sup> They demonstrated, by an inviscid instability analysis, that the surface-piercing wake is, on the whole, convectively unstable, and has an overall form of a recirculation zone terminated by reattachment to the free surface. At the present value of Reynolds number, however, small-scale concentrations of vorticity arising from a convective instability are evident along the edge of the separated shear layer. The swirl patterns of velocity vectors and concentrations of vorticity suggest agglomerations of the smaller scales at sufficiently large distance from the base of the cylinder.

Figure 2(b) shows the effect of cylinder perturbations at three values of excitation frequency  $f = 0.5, 1.0,$  and  $2.0$  Hz and a constant amplitude  $A/D = 0.2$ . The normalized values of excitation frequency, relative to the Kármán frequency  $f_0$  of vortex formation from the completely submerged cylinder, are  $f/f_0 = 0.54, 1.08,$  and  $2.16$ . All images in Fig. 2(b) are taken at the same instant during the oscillation cycle, corresponding to a phase of  $45^\circ$  after attainment of bottom dead center, as described in Sec. II. At each value of excitation frequency  $f$ , comparison of the images in the left and right columns indicates that the structure of the initially formed vortical patterns appear at approximately the same streamwise location, indicating phase-locked vortex formation. At the lowest value of perturbation frequency  $f = 0.5$  Hz, the curved layer of vorticity from the cylinder contacts the free surface and wraps back toward the cylinder, giving the appearance of a large-scale vortex. At a higher value of frequency  $f = 1.0$  Hz, the distribution of vorticity takes on a distinctively different form. A pronounced concentration of vorticity with a well-defined extremum occurs immediately adjacent to the base of the cylinder. On the other hand, at the highest value of  $f = 2.0$  Hz, the initially formed, highly concentrated vortex occurs further downstream, suggesting a change in its timing relative to the motion of the cylinder; this aspect will be addressed subsequently. Viewing the images of Fig. 2(b) as a whole, it is evident that phase-locked, or “locked-in,” vortex formation can be attained over at least a four-fold range of excitation frequency, which is a substantially wider range than for locked-in formation of Kármán vortices from the completely submerged cylinder, as assessed by Griffin and Hall.<sup>10</sup>

## IV. TIMING OF PHASE-LOCKED VORTEX FORMATION

The near-wake structure, in terms of coherent vortex formation adjacent to the free surface, is illustrated in the im-

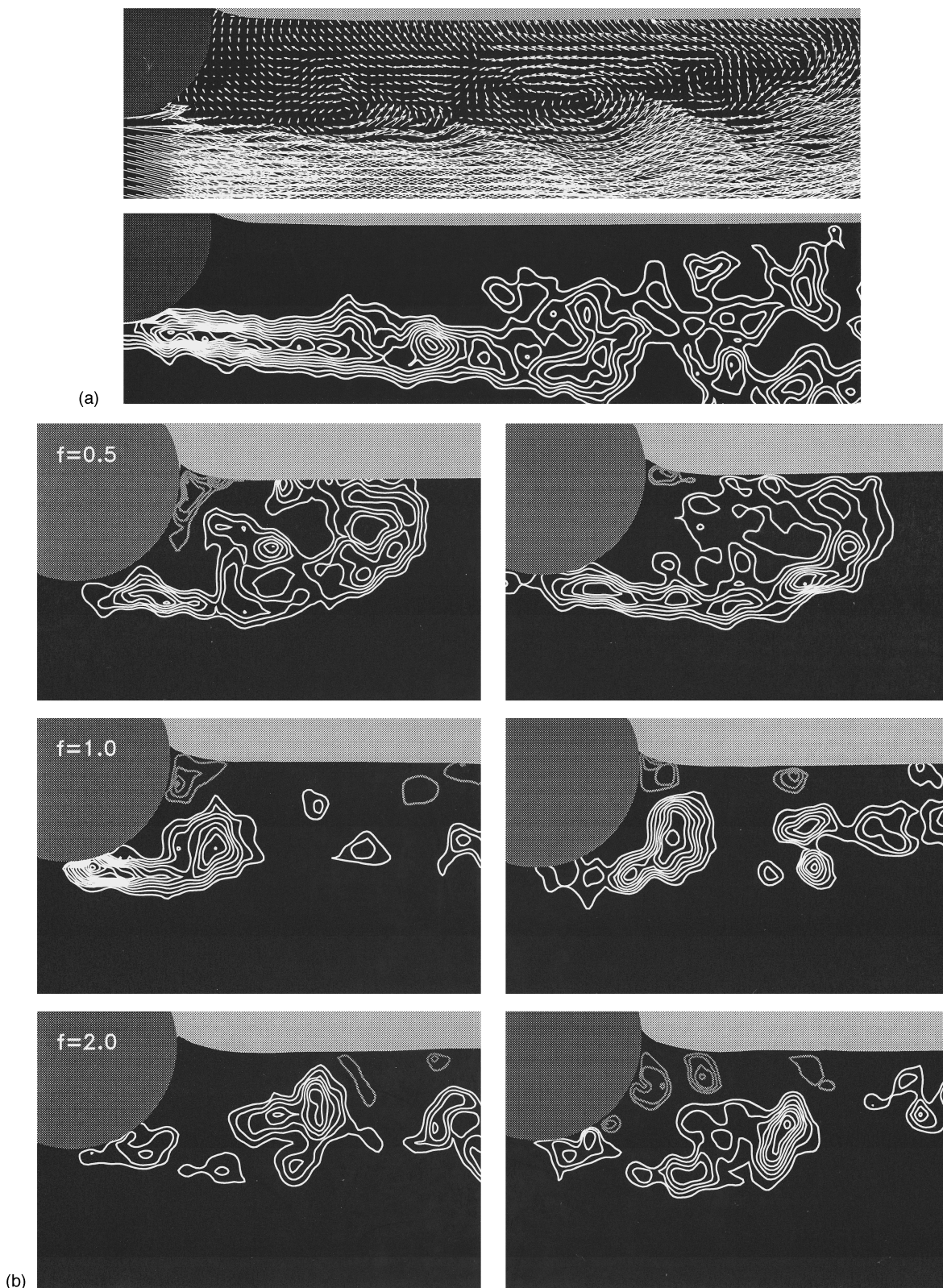


FIG. 2. (a) Ensemble-averaged velocity and vorticity distributions for case of a stationary cylinder. Minimum vorticity contour level is  $|\omega_{\min}|=5 \text{ s}^{-1}$  and incremental vorticity level is  $\Delta\omega=3 \text{ s}^{-1}$ .  $\text{Re}=2855$ . White contours represent positive vorticity in this and all subsequent figures. (b) Instantaneous distributions of vorticity illustrating phase-locked vortex formation during two different cycles of the cylinder motion for indicated values of excitation frequency  $f$  (in Hz). All images correspond to the same instantaneous position, i.e., phase, of cylinder motion. Froude number  $\text{Fr}=0.32$ . Reynolds number  $\text{Re}=2855$ . Dimensionless amplitude  $A/D=0.2$ . Minimum and incremental vorticity contour levels are  $|\omega_{\min}|=12 \text{ s}^{-1}$  and  $\Delta\omega=6 \text{ s}^{-1}$ .

ages of Fig. 3(a) showing instantaneous distributions of velocity, vorticity, and streamline patterns. All images are taken at the same instant during the cylinder oscillation.

At the lowest frequency  $f=0.5$  Hz, the swirl pattern of velocity vectors suggests a region of large-scale vortical activity. The region of highest vorticity, however, occurs at the interface between the free stream and the recirculating flow. In fact, this region accounts for nearly all the circulation; relatively low levels of vorticity and therefore small contributions to the overall circulation, occur within the pattern of swirling velocity vectors. The corresponding streamline pattern shows that well-defined reattachment occurs at the free surface. The reattachment streamline emanates from the irrotational free stream, and not from the surface of the cylinder. The streamline pattern interior to the reattachment streamline exhibits an outward spiral, i.e., an unstable focus. Moreover, a saddle point, indicated by the intersection of streamlines, occurs immediately downstream of separation from the surface of the cylinder.

At a higher value of  $f=0.7$  Hz, a concentrated vortex appears; it is located relatively close to the base of the cylinder. The general features of the velocity distribution and the streamline pattern are the same as those at  $f=0.5$  Hz. A well-defined reattachment point occurs at the free surface and a saddle point exists immediately downstream of separation from the cylinder. The central region of the streamline pattern now exhibits, however, an inward spiral, corresponding to a stable focus, in accord with the enhanced concentration of vorticity.

At  $f=1.0$  Hz, a limiting state of vortex formation is attained. It occurs immediately adjacent to the surface of the cylinder. Correspondingly, the streamline pattern shows the loss of an identifiable saddle point immediately downstream of separation. Moreover, there is no clearly defined, single reattachment point at the free surface. In fact, at a location immediately downstream of the concentrated vorticity, a nodal streamline pattern occurs, with multiple streamlines extending to the free surface. Farther downstream, the pattern of velocity vectors indicates that fluid is ejected downward from the free surface. This pattern is characterized by a nodal streamline parallel and close to the surface. This unusual streamline topology is associated with concentrations of vorticity immediately below the free surface; they were formed at earlier times during the cylinder oscillation.

At the highest value of  $f=2.0$  Hz, the initially formed vortex occurs well downstream of the cylinder, suggesting that it is generated substantially earlier in the oscillation cycle than for the previous cases. In essence, this corresponds to a change in timing of the initially formed vortex, relative to that, for example, at  $f=1.0$  Hz. This change in timing is apparently necessary in order to accommodate the fact that at  $f=1.0$  Hz, the initially formed vortex was forced to occur immediately adjacent to the cylinder; a further increase in excitation frequency cannot draw the vortex farther upstream, rather it occurs at an earlier phase in the oscillation cycle of the cylinder. The streamline topology at  $f=2.0$  Hz shows that the saddle point immediately downstream of separation is again recovered; it occurs closer to the free surface than at  $f=0.71$  and  $0.5$  Hz. The occurrence of a nodal

streamline pattern and multiple reattachment streamlines occur in a similar fashion as at  $f=1.0$  Hz.

For the case of the completely submerged cylinder, Gu, Chyu, and Rockwell<sup>21</sup> interpret the timing of vortex formation in terms of instantaneous concentrations of vorticity corresponding to the Kármán vortices. As the value of frequency is increased, the entire pattern of near-wake vorticity concentrations corresponding to the Kármán vortices moves closer to the base of the cylinder. At a critical value of excitation frequency, the initially formed vortex occurs close to the base of the cylinder and a further increase in frequency causes an abrupt change in timing of the initially formed vortex: it switches from one side of the cylinder to the other. Considering the sequence of images in Fig. 3(a), it is evident that an analogous change in timing of the initially formed vortex occurs. In this case, the critical frequency for which vortex formation occurs adjacent to the base of the cylinder is  $f=1.0$  Hz. At a higher value of frequency represented by  $f=2.0$  Hz, the timing of the vortex formation is dramatically altered, such that the first, fully formed vortex occurs well downstream of the cylinder. We therefore conclude that alternate vortex formation from either side of a cylinder, as it occurs from the fully submerged cylinder, is not necessary for substantial changes in timing of the vortex formation relative to the motion of the cylinder.

Further insight into the near-wake structure is provided by Fig. 3(b), which shows patterns of velocity, vorticity, and streamlines at an instant  $\pi$  out of phase with that of Fig. 3(a). Generally speaking, if the patterns of Fig. 3(a) are indeed associated with formation of a detached, identifiable vortex, then one expects to see such a vortex at a later instant, i.e., farther downstream, in the images of Fig. 3(b).

At  $f=0.5$  Hz, no large-scale vortex is detectable within the field of view. Instead, a layer of vorticity is evident beneath and parallel to the free surface. This observation, in conjunction with the corresponding pattern of Fig. 3(a), suggests that when the excitation frequency is sufficiently low, a detached, agglomerated region of vorticity cannot be attained. The layer of vorticity generated during the downstroke in Fig. 3(a) remains, on the whole, in a distributed form and conforms to the free surface during the upstroke motion of the cylinder. The small-scale concentration of vorticity shown in the lower right of the image at  $f=0.5$  Hz corresponds to a Kelvin–Helmholtz vortex in the separating shear layer; three such concentrations are evident in the interconnected region of vorticity from the surface of the cylinder.

At  $f=0.7$  Hz, on the other hand, a large-scale vortex, resulting from agglomeration of vorticity, is evident at a location well downstream of the cylinder. The streamline pattern indicates that the reattachment point on the free surface is located near the right side of the image. The saddle point, located upstream of the large-scale vortical region, arises from the velocity induced by the upward motion of the cylinder adjacent to that associated with the swirl of the large-scale vortical region.

At  $f=1.0$  Hz, generally similar observations hold, but the large-scale is more clearly defined and formed closer to the base of the cylinder. This vortex is due to the continuous

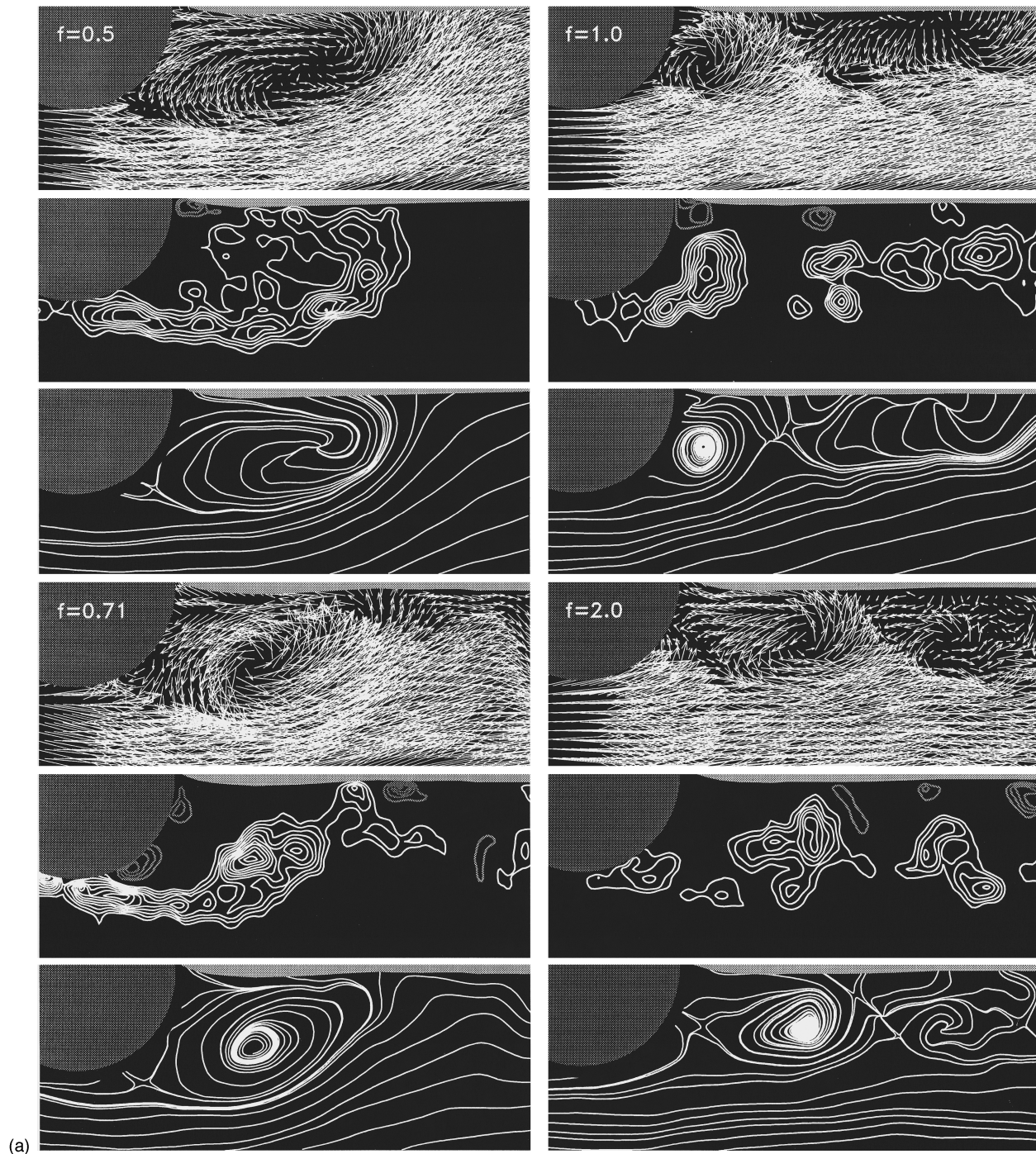


FIG. 3. (a) Instantaneous images of velocity and vorticity fields and streamline patterns for locked-in vortex formation from an oscillating cylinder. All images are at the same instantaneous position, i.e., phase, during the cylinder motion, and correspond to a phase of  $45^\circ$  after attainment of bottom dead center. Excitation frequency is  $f$  (in Hz). Here  $Fr=0.32$ ,  $Re=2855$ . Dimensionless amplitude  $A/D=0.2$ . Minimum and incremental vorticity contour levels are  $|\omega_{\min}|=12 \text{ s}^{-1}$  and  $\Delta\omega=6 \text{ s}^{-1}$ .

feeding of vorticity from the cylinder during the upstroke motion, which combines with the highly concentrated vorticity formed during the downstroke of Fig. 3(a). During the vortex development, however, the topology undergoes a transformation. In Fig. 3(a), the major vortex exhibits an inward spiral (unstable focus), whereas in Fig. 3(b), it has an outward spiral (stable focus).

Finally, at  $f=2.0$  Hz, a concentrated vortex is formed immediately adjacent to the cylinder. This observation is

consistent with the change in timing of the vortex formation discussed in conjunction with Fig. 3(a). Note the similarity of the image at  $f=2.0$  Hz in Fig. 3(b) (upstroke criterion) with that at  $f=1.0$  Hz in Fig. 3(a) (downstroke criterion). The similarity of these patterns, which occur at instants during the oscillation cycle that are shifted by  $\pi$  relative to each other, further reaffirms the change in timing of the initially formed vortex as the frequency is increased from  $f=1.0$  to 2.0 Hz.

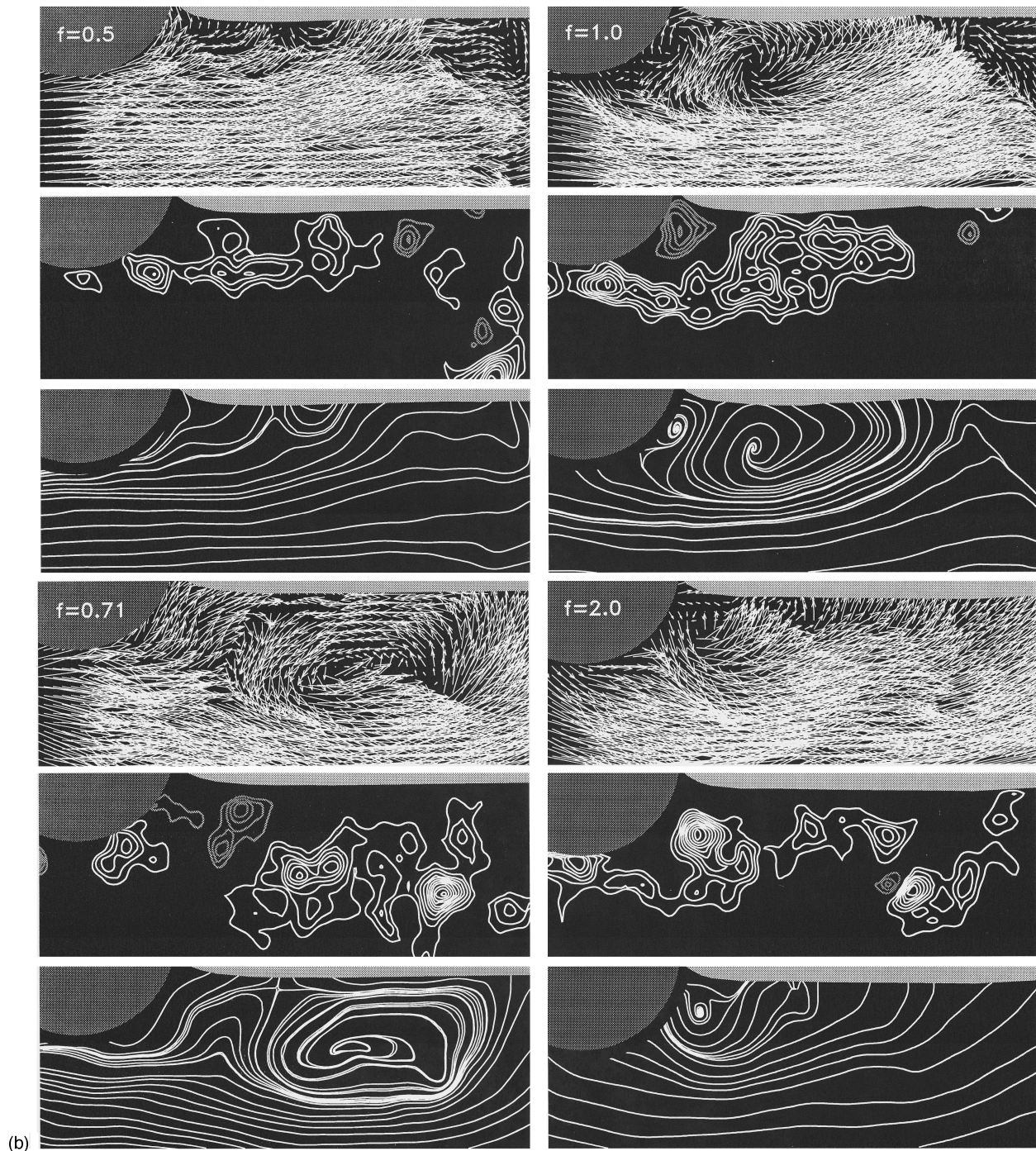


FIG. 3. (b) Matching images for (a) corresponding to a phase  $45^\circ$  after attainment of the top dead center.

An additional point concerns the change in curvature of the region of the free surface adjacent to the oscillating cylinder evident, for example, by comparing the images at  $f=1.0$  in Figs. 3(a) and 3(b). This change in curvature, in conjunction with the formation of the primary vortex from the bottom surface of the cylinder, can give rise to a pronounced concentration of negative (gray) vorticity in that region.

#### V. EFFECT OF AMPLITUDE ON PHASE-LOCKED STATES OF NEAR WAKE

Figure 4 shows the structure of the near wake at two extreme values of excitation frequency  $f=0.67$  and  $2.0$  Hz

for a range of oscillation amplitudes  $A=1, 2,$  and  $5$  mm. All images correspond to the same instantaneous position of the cylinder. At  $f=0.67$  Hz, for the largest amplitude,  $A=5$  mm, a concentrated vortex is clearly formed close to the cylinder. The change in character of the initially formed vortex can be interpreted in terms of reattachment length. At  $A=1$  and  $2$  mm, instantaneous reattachment to the free surface occurs well downstream of the cylinder, whereas at  $A=5$  mm, it has moved upstream a substantial distance to a location closer to the cylinder. At these low amplitudes, the irregular thickening of the shear layer is due to small-scale vorticity concentrations arising from the small-scale Kelvin–Helmholtz in-

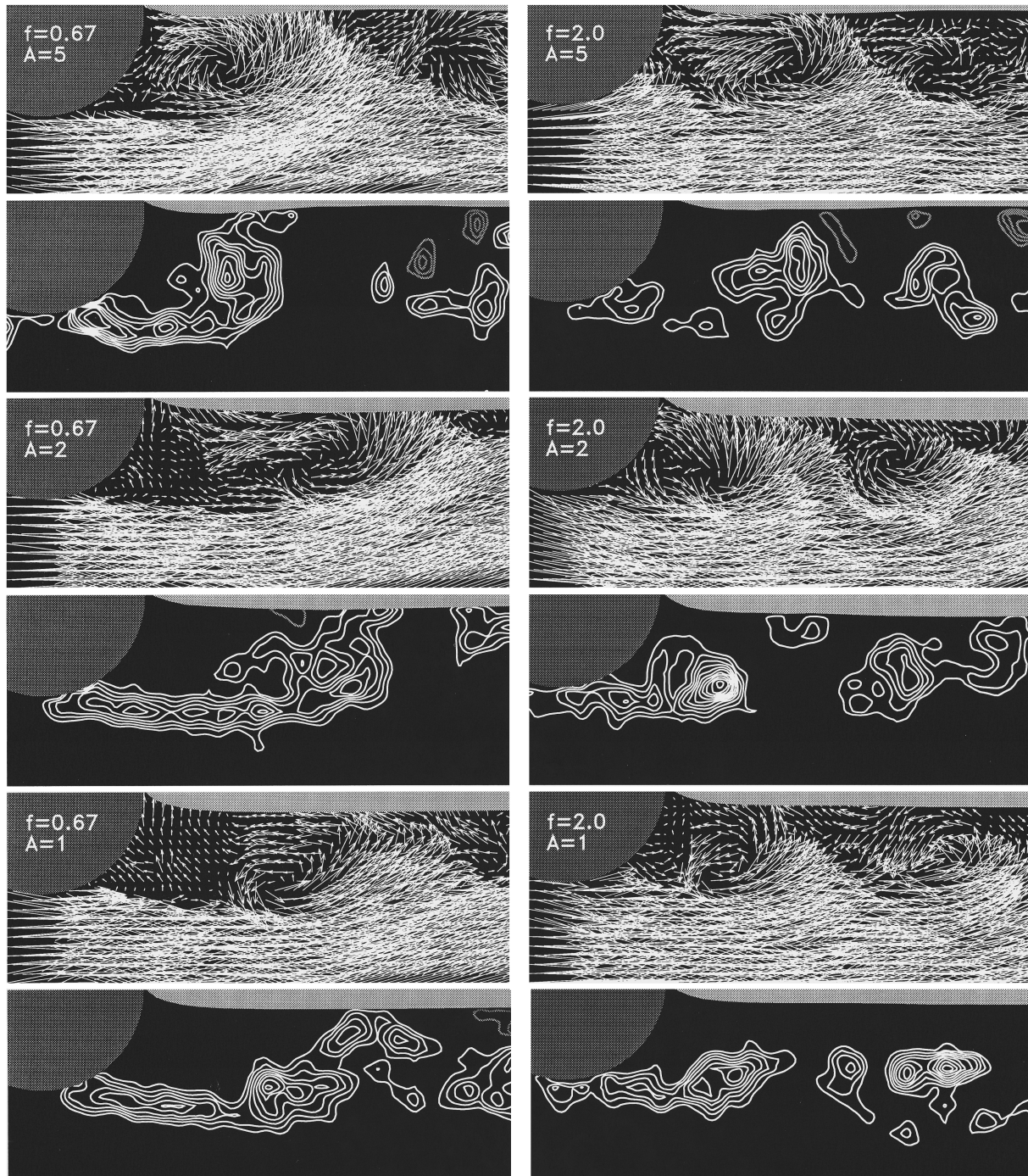


FIG. 4. Instantaneous images of velocity and vorticity fields showing the effect of amplitude  $A$  (in mm) of cylinder oscillation at two values of frequency  $f$  (in Hz). All images are at the same instantaneous position, i.e., of  $45^\circ$  after attainment of the bottom dead center. Here  $Fr=0.32$ ,  $Re=2855$ . Dimensionless amplitudes are  $A/D=0.2$ ,  $0.08$ , and  $0.04$ . Minimum and incremental vorticity contour levels are  $|\omega_{\min}|=12 \text{ s}^{-1}$  and  $\Delta\omega=6 \text{ s}^{-1}$ .

stability. It is therefore apparent that at a given value of excitation frequency, at least in the lower range, formation of a well-defined concentration of vorticity requires a sufficiently large amplitude of excitation. If this threshold value is not attained, then the separated vorticity layer simply curves toward the free surface and forms a recirculation zone between the base of the cylinder and the free surface.

At a sufficiently high value of excitation frequency,  $f=2.0$  Hz, where well-defined concentrations of vorticity are generated over a wide range of amplitude  $A$ , the response of

the vortex patterns is as shown in the right column of Fig. 4. Considering first the lowest amplitude  $A=1$  mm, then  $A=2$  mm, it is evident that this increase in amplitude promotes formation of the vorticity concentration closer to the base of the cylinder. At the largest amplitude,  $A=5$  mm, this trend is broken due to a change in timing of the initially formed vortex. For this case, as already suggested in previous images, the first highly concentrated region of vorticity is formed well downstream of the cylinder, and a low level

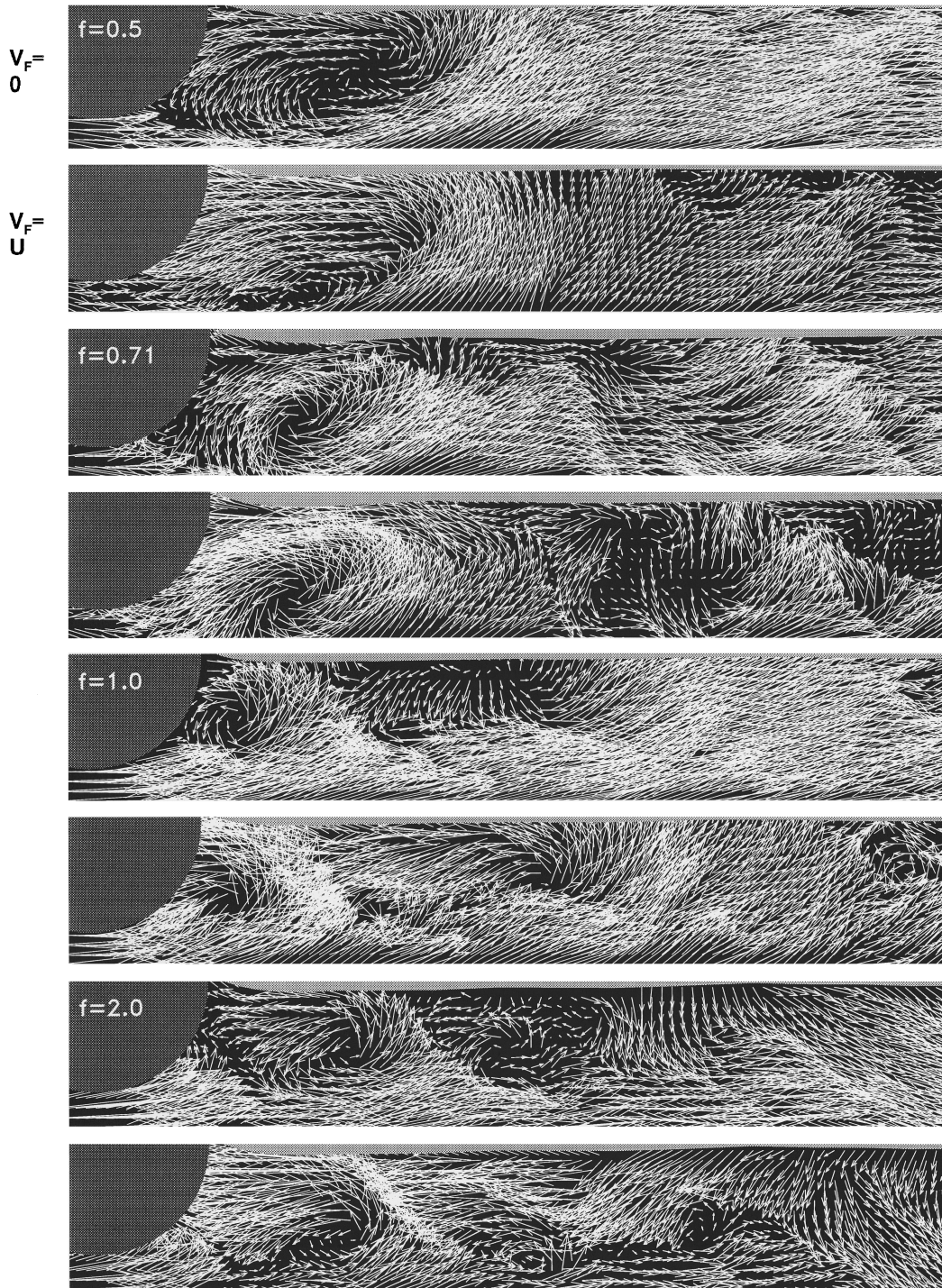


FIG. 5. Instantaneous velocity fields showing the structure of the intermediate wake in relation to the near wake of the oscillating cylinder. Velocity fields are shown in the laboratory reference frame  $V_F=0$  and in a frame moving at the free-stream velocity  $V_F=U$ , for three different values of excitation frequency  $f$  (in Hz). All images are acquired at the same instantaneous position, i.e., a phase of  $45^\circ$  after attainment of the bottom dead center.  $Fr=0.32$ ,  $Re=2855$ . Dimensionless amplitude  $A/D=0.2$ .

concentration exists at the shoulder of the cylinder; it corresponds to the next vortex in the sequence.

## VI. EFFECT OF NEAR-WAKE STRUCTURE ON DOWNSTREAM WAKE

Images showing the relationship between vortical patterns formed in the near wake and the downstream region of

the wake, i.e., the intermediate wake, are shown in Fig. 5. All images are taken at the same instant of the oscillation cycle. At each value of excitation frequency  $f$ , two reference frames are employed. The first, designated as  $V_F=0$ , corresponds to the laboratory frame, and the second, indicated by  $V_F=U$ , is a frame moving with the free-stream vorticity  $U$ . The latter frame is expected to bring out features of the vortical motion. Viewing the images of Fig. 5 as a whole, a

particularly evident feature is the approach of the initially formed vortex toward the base of the cylinder as  $f \rightarrow 1.0$ , which confirms the near-wake observation of Fig. 3(a).

At the lowest frequency,  $f=0.5$  Hz, a swirl pattern is evident in the very near wake at  $V_F=0$ , but much less so at  $V_F=U$ . No vortical patterns are suggested in the downstream wake region. This observation, combined with the lack of any identifiable vortical structures in the downstream region of the wake, along with the patterns of Fig. 3(a), reaffirms the view that only simple “flapping” of the shear layer occurs at this low frequency, rather than its agglomeration into a large-scale vortex. At  $f=0.71$  Hz, for which a clearly defined vortex is evident in both frames  $V_F=0$  and  $U$ , a large-scale vortical pattern is suggested in the downstream region of the wake in the image corresponding to  $V_F=U$ . At  $f=1.0$  and  $2.0$  Hz, for the frame  $V_F=U$ , two successive swirl patterns of velocity vectors are indicated in the region of the wake immediately downstream of the initially formed vortex.

## VII. CONCLUSIONS

A stationary, horizontal cylinder piercing a free surface does not give rise to highly coherent, self-sustained vortex formation in the manner of Kármán vortices from a completely submerged cylinder. The presence of a free surface appears to inhibit the absolute (global) instability, and thereby the mechanism leading to limit cycle oscillations. As shown by the linear stability analysis of Triantafyllou and Dimas,<sup>22</sup> the cylinder-free surface configuration exhibits a convective, rather than an absolute instability, and therefore it is expected to show high sensitivity to applied disturbances. In fact, phase-locked patterns of vortex formation can be generated over a very wide range of excitation frequency at low perturbation amplitudes, relative to the case of the completely submerged cylinder.

At sufficiently high excitation frequency, well-defined concentrations of vorticity are formed from the surface of the cylinder and, as the value of perturbation frequency is increased, the initially formed vortex moves closer to the base of the cylinder until a limiting state is reached, such that vortex formation occurs immediately adjacent to the cylinder surface. A further increase in perturbation frequency induces a dramatic change in timing of the initially shed vortex relative to the cylinder motion. For the case of the completely submerged cylinder, as addressed by Gu, Chyu, and Rockwell,<sup>21</sup> a conceptually similar change in timing of the initially shed concentration of vorticity can occur. The common feature of both the surface piercing and the completely submerged cylinder is attainment of a limiting position of the initially formed vortex immediately adjacent to the base of the cylinder; it is a necessary prelude to the change in timing of the initial vortex. The practical importance of this change in timing is alteration of the direction of energy transfer between the fluid and the cylinder. It is well known, on the basis of the previous studies cited in the Introduction, that the onset of a peak of the fluctuating lift on the cylinder is accompanied by a change in phase between the lift and the cylinder displacement. In turn, these alterations of the load-

ing are accompanied by a switch of the initially formed vortex from one side of the cylinder to the other.

Further distinguishing features of the near wake of the surface-piercing cylinder are revealed by consideration of the instantaneous streamline topology. The occurrence of a saddle point immediately downstream of separation, due to simultaneous existence of flow induced by the motion of the cylinder and the recirculating flow associated with the vortex formation, appears to be unique to the surface-piercing cylinder. Moreover, the occurrence of a well-defined reattachment point at the free surface, at least for moderate values of perturbation frequency, is another feature that is not present for the wake of a completely submerged cylinder. This reattachment to the free surface produces a confined region of intensely recirculating (swirling) flow between the reattachment streamline, the free surface, and the base of the cylinder. Although the patterns of velocity vectors and streamlines suggest the existence of a large-scale vortex in this region, it has been demonstrated that, at low values of excitation frequency, the major share of the vorticity is along a locus coincident with a trajectory of the separating layer from the cylinder, rather than distributed throughout the circulation region. At sufficiently high excitation frequency, however, rapid agglomeration of vorticity is attainable, and the patterns of velocity vectors and streamlines accurately indicate a concentration of vorticity.

## ACKNOWLEDGMENTS

The authors gratefully acknowledge support of the Office of Naval Research, Grants No. N00014-94-1-0185 and No. N00014-94-1-1183, monitored by Dr. Thomas Swean.

<sup>1</sup>G. H. Koopman, “The vortex wakes of vibrating cylinders at low Reynolds numbers,” *J. Fluid Mech.* **28**, 501 (1967).

<sup>2</sup>G. H. Koopman, “On the wind-induced vibrations of circular cylinders,” M.Sc. thesis, Catholic University of America, Washington, D.C., 1967.

<sup>3</sup>O. M. Griffin, “The unsteady wake of an oscillating cylinder at low Reynolds number,” *Trans. ASME J. Appl. Mech.* **38**, 729 (1971).

<sup>4</sup>O. M. Griffin, “Instability in the vortex street wakes of vibrating bluff bodies,” *Trans. ASME J. Fluid Eng.* **95**, 569 (1973).

<sup>5</sup>O. M. Griffin and C. W. Vortaw, “The vortex street in the wake of a vibrating cylinder,” *J. Fluid Mech.* **51**, 31 (1972).

<sup>6</sup>A. Ongoren and D. Rockwell, “Flow structure from an oscillating cylinder. Part 1. Mechanisms of phase shift and recovery of the near-wake,” and “Flow structure from an oscillating cylinder. Part 2. Mode competition in the near-wake,” *J. Fluid Mech.* **191**, 197 (1988).

<sup>7</sup>M. Cheng and P. M. Moretti, “Lock-in phenomena on a single cylinder with forced transverse vibration,” *Flow-Induced Vibrations and Wear 1991* (ASME, New York, PVP-206, p. 129).

<sup>8</sup>C. H. K. Williamson and A. Roshko, “Vortex formation in the wake of an oscillating cylinder,” *J. Fluid Struct.* **2**, 355 (1988).

<sup>9</sup>O. M. Griffin and M. S. Hall, “Vortex shedding lock-on and flow control in bluff body wakes,” *Trans. ASME, J. Fluid Eng.* **113**, 526 (1991).

<sup>10</sup>O. M. Griffin and M. S. Hall, “Vortex shedding lock-on in a circular cylinder wake,” *Flow-Induced Vibration*, edited by P. W. Bearman, p. 3.

<sup>11</sup>R. E. D. Bishop and A. Y. Hassan, “The lift and drag forces on a circular cylinder oscillating in a flowing fluid,” *Proc. R. Soc. London Ser. A* **277**, 51 (1964).

<sup>12</sup>T. Staubli, “Calculation of the vibration of an elastically mounted cylinder using experimental data from a forced oscillation,” *ASME Symposium on Fluid-Structure Interaction in Turbomachinery*, 1981, Vol. 19.

- <sup>13</sup>T. Sarpkaya, "Fluid forces on oscillation cylinders," *J. Waterways Ports Coastal Ocean Div. ASCE* **104**, 275 (1978).
- <sup>14</sup>P. W. Bearman and E. G. Currie, "Pressure fluctuation measurements on an oscillating circular cylinder," *J. Fluid Mech.* **91**, 661 (1979).
- <sup>15</sup>M. Ferguson and G. V. Parkinson, "Surface and wake flow phenomena of the vortex-excited oscillation of the circular cylinder," *Trans. ASME B: J. Eng. Ind.* **89**, 831 (1967).
- <sup>16</sup>C. C. Feng, "The measurement of vortex-induced effects on flow past stationary and oscillating circular and D-section cylinders," M.A.Sc. thesis, University of British Columbia, 1968.
- <sup>17</sup>P. W. Bearman and E. D. Obasaju, "An experimental study of pressure fluctuations on fixed and oscillating square-section cylinders," *J. Fluid Mech.* **119**, 297 (1982).
- <sup>18</sup>T. Staubli and D. Rockwell, "Pressure fluctuations on an oscillating trailing edge," *J. Fluid Mech.* **203**, 307 (1989).
- <sup>19</sup>A. Lotfy and D. Rockwell, "The near-wake of an oscillating trailing-edge: Mechanisms of periodic and aperiodic response," *J. Fluid Mech.* **251**, 173 (1993).
- <sup>20</sup>M. M. Zdravkovich, "Modification of vortex shedding in the synchronization range," *Trans. ASME I J. Fluid Eng.* **104**, 513 (1982).
- <sup>21</sup>W. Gu, C. Chyu, and D. Rockwell, "Timing of vortex formation from an oscillating cylinder," *Phys. Fluids* **6**, 3677 (1994).
- <sup>22</sup>G. S. Triantafyllou and A. A. Dimas, "Interaction of two-dimensional separated flows with a free surface at low Froude Numbers," *Phys. Fluids A* **1**, 1813 (1989).
- <sup>23</sup>G. S. Triantafyllou and A. A. Dimas, "The low Froude number wake of floating bluff objects," Internal Report No. MITSG 89-5, Massachusetts Institute of Technology, Cambridge, 1989.
- <sup>24</sup>D. Rockwell, C. Magness, J. Towfighi, O. Akin, and T. Corcoran, "High-image-density particle image velocimetry using laser scanning techniques," *Exp. Fluids* **14**, 181 (1993).